Title

Two subunits of the exocyst, Sec3p and Exo70p, can function exclusively on the plasma membrane

Journal

Molecular Biology of the Cell, 29(6)

ISSN

1059-1524

Authors

Liu, Dongmei
Li, Xia
Shen, David
et al.

Publication Date

2018-03-15

DOI

10.1091/mbc.e17-08-0518

Peer reviewed

Two subunits of the exocyst, Sec3p and Exo70p, can function exclusively on the plasma membrane

Dongmei Liu, Xia Li, David Shen, and Peter Novick*
Department of Cellular and Molecular Medicine, University of California, San Diego, La Jolla, CA 92130

ABSTRACT **The exocyst is an octameric complex that tethers secretory vesicles to the plasma membrane in preparation for fusion. We anchored each subunit with a transmembrane (TM) domain at its N- or C-terminus. Only N-terminally anchored TM-Sec3p and C-terminally anchored Exo70p-TM proved functional. These findings orient the complex with respect to the membrane and establish that Sec3p and Exo70p can function exclusively on the membrane. The functions of TM-Sec3p and Exo70p-TM were largely unaffected by blocks in endocytic recycling, suggesting that they act on the plasma membrane rather than on secretory vesicles. Cytosolic pools of the other exocyst subunits were unaffected in *TM-sec3* cells, while they were partially depleted in *exo70-TM* cells. Blocking actin-dependent delivery of secretory vesicles in *act1-3* cells results in loss of Sec3p from the purified complex. Our results are consistent with a model in which Sec3p and Exo70p can function exclusively on the plasma membrane while the other subunits are brought to them on secretory vesicles.**

Monitoring Editor
Akihiko Nakano
RIKEN

Received: Aug 18, 2017
Revised: Jan 9, 2018
Accepted: Jan 10, 2018

INTRODUCTION

Vesicular traffic is used to transport material between the various compartments of the exocytic and endocytic pathways. Each stage of transport requires the selective incorporation of cargo from a donor compartment into vesicular carriers followed by the accurate targeting of those vesicles to an appropriate acceptor compartment. Recognition of the acceptor compartment by the vesicle involves several components that act sequentially. Tethers form the initial link, binding to the cytoplasmic surface of both the vesicle and the acceptor compartment (Brown and Pfeffer, 2010). Known tethers include both long coiled-coil molecules as well as multi-subunit complexes (Yu and Hughson, 2010). Most multi-subunit tethers contain components that share a common structural feature: helical bundles linked in series to generate a rod-like element (Dong *et al.*, 2005; Tripathi *et al.*, 2009; Vasan *et al.*, 2010). After vesicle-target recognition by the tether, a SNARE complex, involving membrane-anchored components on both the vesicle (vSNARE) and target compartment (tSNARE), is assembled. SNARE complex assembly provides an additional layer of specificity to the targeting reaction and drives membrane fusion (McNew *et al.*, 2000). Several lines of evidence suggest that tethers provide more than a passive linkage between the vesicle and acceptor compartment and can play an active role in catalyzing SNARE complex assembly (Ren *et al.*, 2009; Yue *et al.*, 2017).

Here we focus on the exocyst, a large, conserved, multi-subunit tethering complex required for fusion of secretory vesicles with the plasma membrane at sites of polarized cell surface growth. All eight subunits (Sec3p, Sec5p, Sec6p, Sec8p, Sec10p, Sec15p, Exo70p, and Exo84p) are present at one copy per complex (TerBush *et al.*, 1996). In yeast, all but one of the structural genes are essential and, while deletion of *SEC3* is not lethal, *sec3*Δ cells grow very slowly at 25°C, and above 30°C growth is blocked (Finger and Novick, 1997). Several exocyst subunits interact with components on the vesicle surface; Sec15p binds to the GTP-bound form of the secretory vesicle-associated Rab GTPase, Sec4p (Guo *et al.*, 1999), while Sec6p binds to the vSNARE, Snc1p (Shen *et al.*, 2013). In addition, several subunits interact with components on the cytoplasmic face of the plasma membrane. The amino-terminal domain of Sec3p and the carboxy-terminal domain of Exo70p bind $PI(4,5)P_2$ (He *et al.*, 2007; Zhang *et al.*, 2008), a lipid predominantly associated with the cytoplasmic leaflet of the plasma membrane. The amino-terminal domain of Sec3p also binds to Cdc42p and Rho1p (Guo *et al.*, 2001; Zhang *et al.*, 2001) while Exo70p binds to Cdc42p and Rho3p, all members of the Rho GTPase family that play key roles in polarity

This article was published online ahead of print in MBoC in Press (http://www.molbiolcell.org/cgi/doi/10.1091/mbc.E17-08-0518) on January 17, 2018.

*Address correspondence to: Peter Novick (pnovick@ucsd.edu).

Abbreviations used: 5′-FOA, 5-fluoroorotic acid; DTT, dithiothreitol; ER, endoplasmic reticulum; GFP, green fluorescent protein; HA, hemagglutinin; PIPES, piperazine-*N*,*N*′-bis(2-ethanesulfonic acid); PMSF, phenylmethanesulfonyl fluoride; RT, room temperature; SC, synthetic complete; WT, wild type; YPD, yeast peptone dextrose.

establishment at the cell cortex. In addition, Exo70p also binds to the cortical polarity scaffold protein Bem1p (Liu and Novick, 2014), while Sec6p binds to the tSNARE, Sec9p, the assembled SNARE complex (Dubuke *et al.*, 2015) and the SNARE regulator, Sec1p (Morgera *et al.*, 2012). Collectively, these interactions serve to link incoming secretory vesicles to specialized sites on the plasma membrane, defined by the cell polarity machinery, in preparation for exocytic fusion. Recently an interaction of Sec3p with the Sso2p tSNARE has been implicated in catalyzing assembly of the Sso-Sec9 binary tSNARE complex (Yue *et al.*, 2017).

At steady state, all components of the exocyst are concentrated at sites of polarized cell surface growth (TerBush and Novick, 1995; Finger *et al.*, 1998; Boyd *et al.*, 2004). These include the tips of small buds early in the cell cycle and the necks of large budded cells near the time of cytokinesis. Most components of the exocyst arrive at these sites by riding on secretory vesicles as they are delivered along polarized actin cables by the type V myosin, Myo2p, and thus their polarized localization is sensitive to the disruption of actin filaments by latrunculin A or by mutations in tropomyosin (Finger *et al.*, 1998; Boyd *et al.*, 2004). Several studies have found that the localization of Sec3p and Exo70p is at least partially resistant to these conditions but sensitive to the loss of Cdc42p or Rho function (Guo *et al.*, 2001; Zhang *et al.*, 2001). The actin-independent localization of Exo70p relies on its interaction with the polarity scaffold protein, Bem1p (Liu and Novick, 2014). These findings have led to the proposal that the exocyst may undergo cycles of assembly and disassembly in which most components ride on vesicles to polarized exocytic sites at the cell cortex that are marked by Sec3p and Exo70p (Boyd *et al.*, 2004). Exocyst assembly would then serve to tether the incoming vesicle to these sites. Disassembly would presumably be required for additional rounds of function. Aspects of this model have been questioned. One study found that Sec3p localization, like that of the other subunits, is sensitive to the disruption of actin filaments (Roumanie *et al.*, 2005) while another failed to detect the pool of partially assembled exocyst subcomplexes predicted by the model (Heider *et al.*, 2016). Here we explore several aspects of exocyst function relating to these issues. To evaluate the requirement for the cytosolic and vesicular pools of the exocyst, we determine if the exocyst can fulfill all of its essential functions when irreversibly anchored to the plasma membrane. We also determine the effects of a temperature-sensitive mutation in the actin structural gene on exocyst assembly and stability.

RESULTS

Sec3p is the only exocyst subunit that can function when anchored to the membrane through an N-terminal transmembrane domain

To assess the effects of anchoring exocyst subunits to the membrane, we first fused the TM domain from Tos2p to the N-terminus of each exocyst component, individually. Tos2p contains a single predicted transmembrane (TM) domain within its N-terminal region and localizes to polarized growth sites, such as the bud cortex in small-budded cells and as a double-ring structure at the bud neck in large-budded cells (Drees *et al.*, 2001; Gandhi *et al.*, 2006). This localization resembles that of the exocyst complex and colocalization is seen at bud tips or bud necks in about two thirds of cells expressing both Tos2p-3xGFP (green fluorescent protein) and Sec6p-2xmCherry (Supplemental Figure S1). To allow for the possibility that adding a TM domain to an exocyst subunit would cause loss of function and thus impair cell viability, we introduced the Tos2TM (amino acids 2–74) to one copy of each gene locus in the presence of either a balancing wild-type (WT) copy (in a diploid strain or on a *URA3*, CEN vector) or a high copy number bypass suppressor. To reveal the phenotype, the balancing copy of the exocyst gene or the suppressor plasmid was removed, either by sporulation and tetrad dissection or by selection against the Ura3 plasmid by growth on 5-fluoroorotic acid (5′-FOA).

In the case of Sec3p, we introduced a CEN vector that expresses Tos2$^{2\text{-}74}$-Sec3p-4xHA (hemagglutinin) into a *sec3*Δ strain that was complemented with WT *SEC3* on a *URA3*, CEN vector (NY3237). After the balancing plasmid was removed, the resulting yeast strain had only one copy of *SEC3* and it was fused to the *tos2TM* domain at its N-terminus. Deletion of *SEC3* is not lethal; however *sec3*Δ strains grow very slowly at 25°C and fail to grow at temperatures above 30°C (Finger and Novick, 1997). In contrast, strains expressing *tos2TM-sec3-4xHA* grow similarly to WT (Figure 1A). To confirm the result and to exclude the possibility of an extragenic suppressor, we backcrossed the strain to WT (NY1210) and performed growth tests with the resulting progeny. Some of the *tos2TM-sec3-4xHA* spores were slightly smaller than their WT counterparts (Figure 1B) and showed a growth rate similar to WT at 34° and 37°C but somewhat slower growth at 25° and 30°C (Figure 1C).

We further performed secretion assays to analyze the efficiency of vesicular transport in the *TM-sec3* mutant strain. Invertase and Bgl2p are delivered to the cell surface through two distinct populations of secretory vesicles (Harsay and Bretscher, 1995). As shown in Supplemental Figure S2, at 37°C *TM-sec3* accumulated a slightly larger-than-normal internal pool of both invertase (8% vs. 1%) and Bgl2p (4% vs. 3%). However, in comparison with *sec6-4*, a well-known exocyst mutant with a severe secretion defect or various alleles of *SEC3* (Finger and Novick, 1997), this effect was negligble. Consistent with the growth test results (Figure 1C), the *TM-sec3* strain accumulated a slightly larger internal pool of Bgl2p at 25°C than at 37°C (6% vs. 4%). These data indicate that adding a transmembrane domain to the N-terminus of Sec3p does not seriously diminish its function.

Using a similar approach, we tested the effect of anchoring Exo70p by taking advantage of the fact that the lethality of *exo70*Δ can be rescued by overexpression of *SEC1* (Wiederkehr *et al.*, 2004). After introducing a tos2TM-Exo70 construct into an *exo70*Δ strain, we tested the ability of the strain to survive without the *SEC1* plasmid. Unlike the situation with Sec3p, adding Tos2TM to the amino terminus of Exo70p proved lethal to the cells, as did loss of *EXO70* (Figure 1D).

For the other six exocyst subunits, Sec5p, Sec6p, Sec8p, Sec10p, Sec15p, and Exo84p, as they are all essential for cell viability, we introduced Tos2TM to the N-terminus of one copy of the exocyst open reading frame tagged with an HA or myc tag at the C-terminal end to facilitate detection, while keeping another intact WT copy as a balancer in a diploid strain (Figure 1E). Tetrad dissection was performed to obtain spores expressing, as the sole copy, exocyst subunits fused at their N-termini to Tos2TM (Figure 1F). For all tetrads resulting from the dissection of *tos2TM-sec5/SEC5*, *tos2TM-sec6/SEC6*, *tos2TM-sec8/SEC8*, *tos2TM-sec10/SEC10*, and *tos2TM-sec15/SEC15* diploids, there were two viable spores and two dead spores. Since all the viable spores were WT, the dead spores would have expressed Tos2TM fused to the N-terminus of the exocyst subunit. In the case of the *tos2TM-exo84/EXO84* dissection, although there were two viable *tos2TM-exo84* spores in most tetrads, they were very small and grew too slowly to propagate and analyze. Therefore, among this group, we have only focused on *tos2TM-sec3* in the following studies and consider Sec3p to be the only subunit that can function effectively with an N-terminal TM domain.

To further test whether Tos2TM-Sec3p is stably anchored to the membrane, we performed subcellular fractionation by differential

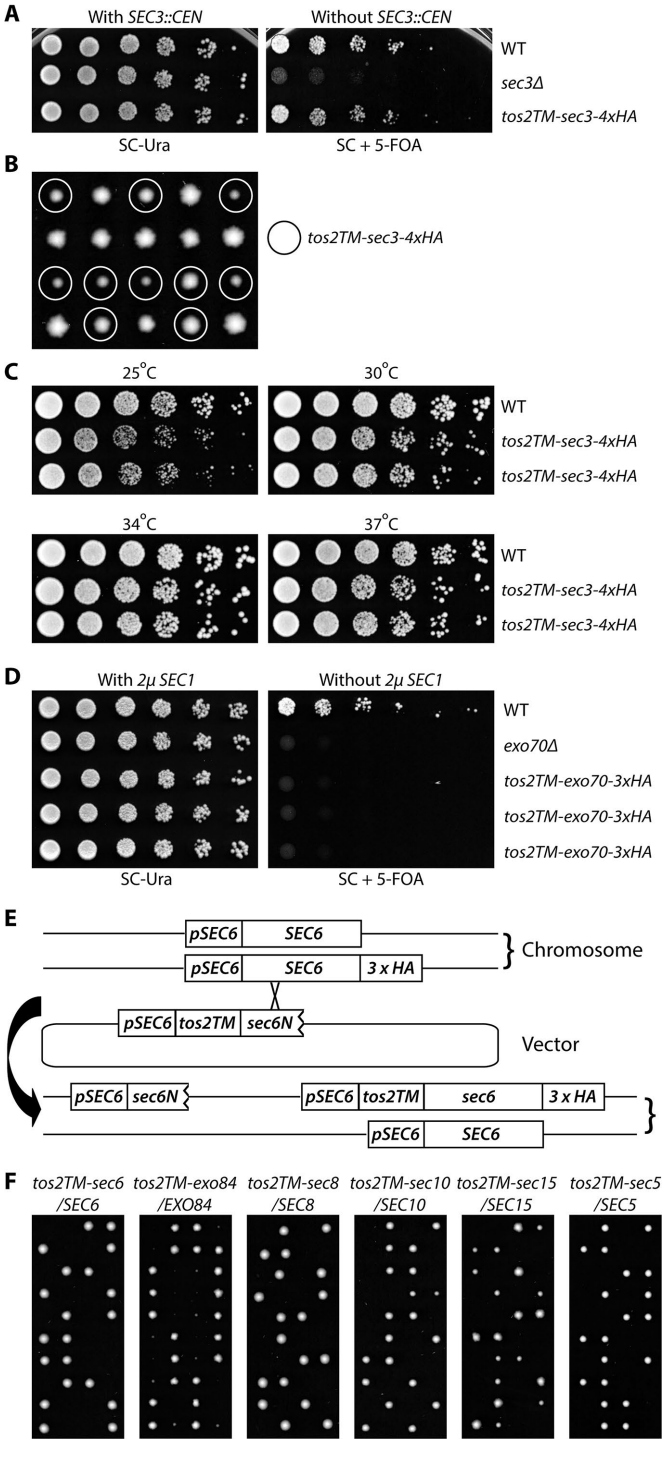

FIGURE 1: Sec3p is the only exocyst subunit that can function when anchored to the membrane through an N-terminal transmembrane (TM) domain (A) WT, *sec3*Δ, and *tos2TM-sec3-4xHA* yeast strains with a complementing *SEC3* CEN URA vector (NY3298, NY3236, and NY3237) were grown to early log phase in SC-Ura liquid medium at 25°C, serially diluted, and spotted on SC-Ura or SC with 5′-FOA. The plates were then incubated for 3 d at 25°C. (B) Yeast strain *tos2TM-sec3-4xHA* was backcrossed to WT NY1210. Diploid yeast cells were sporulated and dissected on YPD plates, then spores were incubated for 4 d at 25°C. Mutant spores (*tos2TM-sec3-4xHA*) are marked with circles. (C) Two mutant spores of *tos2TM-sec3-4xHA* obtained from the above dissection were grown to early log phase in YPD medium at 25°C, serially diluted, and spotted on YPD plates. The plates were then incubated for 2 d at 25°C, 30°C, 34°C, and 37°C, respectively. (D) WT, *exo70*Δ, and *tos2TM-exo70-3xHA* yeast strains carrying a *SEC1* 2μ *URA3* vector (NY3239, NY2478, and NY3240) were grown to early log phase in SC-Ura liquid medium at 25°C, serially diluted, and spotted on SC-Ura or SC with 5′-FOA. The plates were then incubated for 3 d at 25°C. (E) Schematic representation of the approach used to generate *tos2TM-sec6-3xHA*. Similar approaches were used for *EXO84*, *SEC8*, *SEC10*, *SEC15*, and *SEC5*. A yeast strain with 3xHA at the C-terminal end of *SEC6* was crossed with WT. The resulting diploid strain was transformed with a vector containing the *SEC6* promoter, *tos2TM*, and a short, N-terminal fragment of *SEC6*. Transformants in which recombination had occurred with the HA-tagged chromosomal copy were selected by PCR. The selected diploid was then sporulated and tetrads were dissected on YPD plates, which were incubated for 4 d at 25°C. (F) Diploid strains as indicated (NY3243, 3245-3248, 3250) were sporulated and tetrads were dissected on YPD plates, which were then incubated for 4 d at 25°C.

centrifugation. We subjected lysates to centrifugation at 50,000 × *g* to resolve the membrane bound exocyst pool from the soluble pool. We chose this speed rather than 100,000 × *g* because the assembled exocyst complex is so large (19.5S) that a portion of the soluble pool will sediment at the higher speed (Bowser *et al.*, 1992). As shown in Figure 2A, Tos2TM-Sec3p-4xHA is almost completely excluded from the 50,000 × *g* supernatant. In contrast, WT Sec3p-4xHA has a significant fraction that distributes into the 50,000 × *g* supernatant. A plasma membrane marker, Sso1p, or a secretory vesicle marker Snc1p are found exclusively in the 50,000 × *g* pellet. This confirms that fusing Tos2TM to the N-terminus of Sec3p stably anchors it to the membrane. Since this construct functions quite effectively, with no evidence of proteolytic cleavage (Supplemental Figure S3, lane 3) we conclude that the cytosolic pool of Sec3p is largely, if not entirely dispensable.

All N-terminally anchored exocyst subunits are well expressed

The failure of most exocyst subunits to function when fused at their N-termini to the Tos2TM could be due to either their irreversible association with the plasma membrane, a lack of expression, or failure to exit the endoplasmic reticulum (ER). We evaluated the expression of Tos2TM-Sec3p as the sole copy and the other Tos2TM-tagged exocyst subunits expressed in the presence of either a bypass suppressor (*SEC1*) or a WT balancer copy. As shown in Figure 2, B and C, all of the exocyst subunits fused at their N-termini to Tos2TM were expressed at roughly equivalent levels, except for Tos2TM-Exo84p, which was expressed at a somewhat lower level. We used both immunofluorescence microscopy and subcellular fractionation to assess the extent to which the nonfunctional Tos2TM-anchored constructs were able exit the ER and reach the plasma membrane. In five of seven cases, we were able to detect the tagged constructs by immunofluorescene (Supplemental Figure S4), and in each case we observed either localization to the cell cortex or concentration at cortical sites of polarized growth. No association with the nuclear envelope, indicative of ER retention, was evident. We also used differential centrifugation to resolve the ER from the plasma membrane. Following gentle lysis, the ER marker Sec61p largely sediments at 3000 × *g* while the plasma membrane marker Sso1/2p remains largely in the supernatant (Supplemental Figure S5). Tos2TM-anchored Exo70p, Exo84p, and Sec15p were found predominantly in the 3000 × *g* supernantant, while Tos2TM-anchored Sec8p and Sec10p were about equally split between the supernatant and pellet. Only Tos2TM-anchored Sec5p and Sec6p showed a larger fraction in the 3000 × *g* pellet, yet in both of these cases immunofluorescence indicated association with the cell

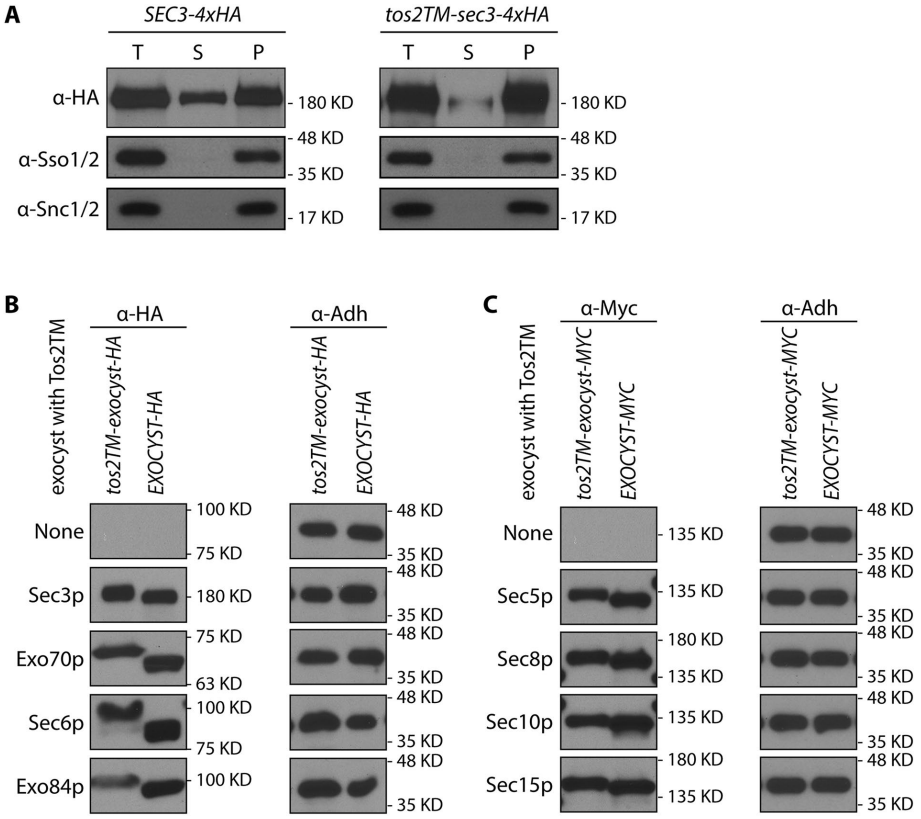

FIGURE 2: (A) Sec3p with an N-terminal TM anchor was largely absent from the 50,000 × *g* supernatant. Total cell lysates (T) from WT (NY2128; left panel) and the *tos2TM-sec3-4xHA* mutant (NY3238; right panel) were centrifuged at 50,000 × *g* for 20 min, separated into supernatant (S) and pellet (P) fractions, and then analyzed by Western blot analysis on a 6% SDS–PAGE gel with anti-HA antibody, anti-Sso1/2, or anti-Snc1/2 serum. (B, C) All exocyst subunits fused at their N-termini to tos2-TM were expressed well. The expression of all exocyst subunits fused at their N-termini to tos2-TM and tagged at their C-termini to either HA (Sec3p, Exo70p, Sec6p, Exo84p) or myc (Sec5p, Sec8p, Sec10p, Sec15p) tail were examined by western blot using either anti-HA or anti-myc antibody. All strains are heterozygous diploids except for *tos2TM-sec3-4xHA*, which is viable as a homozygous haploid, and *tos2TM-exo70-3xHA*, which contains a 2μ *SEC1* plasmid to bypass the requirement of the essential *EXO70* gene. All WT counterparts are haploids expressing an exocyst subunit tagged with either HA or myc tag as indicated. Adh1p was used as a loading control.

periphery rather than the ER (Supplemental Figure S4). The somewhat greater low-speed sedimentation of Tos2TM-anchored Sec5p and Sec6p relative to the others may reflect the greater fraction of the plasma membrane marker that pelleted at low speed in these strains (Supplemental Figure S5). After normalizing for the distribution of Sso1/2p, all Tos2TM-tagged subunits showed a predominant cofractionation with the plasma membrane (Supplemental Figure S5). Thus, it appears unlikely that the failure of these constructs to function is due to a failure to exit the ER.

Exo70p is the only exocyst subunit that can function when anchored to the membrane through a C-terminal TM domain

The various exocyst subunits presumably have a preferred orientation with respect to the membrane. This preference might allow them to function when anchored at their C-termini even if they were found to be nonfunctional when anchored at their N-termini. To explore this possibility, we added a carboxy-terminal TM tail to all eight exocyst subunits. Sso1p is a tail-anchored t-SNARE of the syntaxin family that is predominantly located on the plasma membrane. It forms a complex with Sec9p and the v-SNARE Snc2p that functions in exocytosis (Aalto *et al.*, 1993). We used the Sso1p C-terminal region from amino acids 257–290, which includes a short hydrophilic linker (amino acids 257–265), a single transmembrane domain (amino acids 266–287), and a short extracellular tail (amino acids 288–290), as a C-terminal anchor to attach to each of the eight exocyst subunits. Since adding a TM tail to an exocyst subunit might impair its essential function, we integrated, by homologous recombination, an N-terminally truncated, C-terminally anchored construct into a WT diploid yeast strain to fuse the Sso1TM onto one full-length copy of the exocyst gene and leave the other WT copy intact as a balancer (Figure 3A). Except in the case of *exo70-sso1TM/EXO70*, sporulation and tetrad dissection of all diploid strains yielded two viable colonies and two inviable spores (Figure 3B). In all seven of these dissections the two viable spores proved to be WT, indicating that C-terminally anchoring any exocyst subunit other than Exo70p to the membrane is severely detrimental to its function. Dissection of the *exo70-sso1TM/EXO70* diploid yielded two large and two small progeny from each tetrad. Large colonies proved to be WT while the small ones expressed Exo70p-Sso1TM (Figure 3B, second panel from left). This indicates that Exo70p can function when irreversibly anchored to the membrane through its C-terminus. Growth tests at 25°C confirmed that the *exo70-2xHA-sso1TM* strain is viable, although with a slower growth rate than WT (Figure 3C).

We next tested whether increased expression of Sec3p-Sso1TM could restore viability and whether increased expression of Exo70p-Sso1TM could improve its function. When we expressed Sec3p-4xHA-Sso1TM from the *ADH1* promoter as the sole copy of *SEC3*, the cells were inviable (Figure 3D, top right panel rows 5 and 6), suggesting that lethality was not due to insufficient expression. In fact, expression of Sec3p-4xHA-Sso1TM, either at normal or elevated levels, appears to have an inhibitory effect since the *sec3*Δ strain grew, albeit slowly, at 25°C (Figure 3D, top right panel rows 2–4), while cells expressing Sec3p-4xHA-Sso1TM did not. Expression of Exo70p-2xHA-Sso1TM from the *ADH1* promoter yielded a modest improvement in cell growth relative to strains expressing it from the endogenous promoter (compare Figure 3, D, bottom right panel row 6, and C, row 2). Western blotting confirmed that, relative to its own promoter, the *ADH1* promoter did induce a much higher expression level of *exo70-2xHA-sso1TM* (Figure 3E, lanes 2 and 3 vs. lanes 4 and 5). The increased level of expression appears similar to that of WT *EXO70* expression from its own promoter (Figure 3E, lanes 4 and 5 vs. lane 8); however, due to differences in the copy number of HA tags and the position of the tags within the protein, it is difficult to make a direct comparison between WT and mutants of *exo70*. There was no evidence of proteolytic cleavage products (Supplemental Figure S3, lane 7).

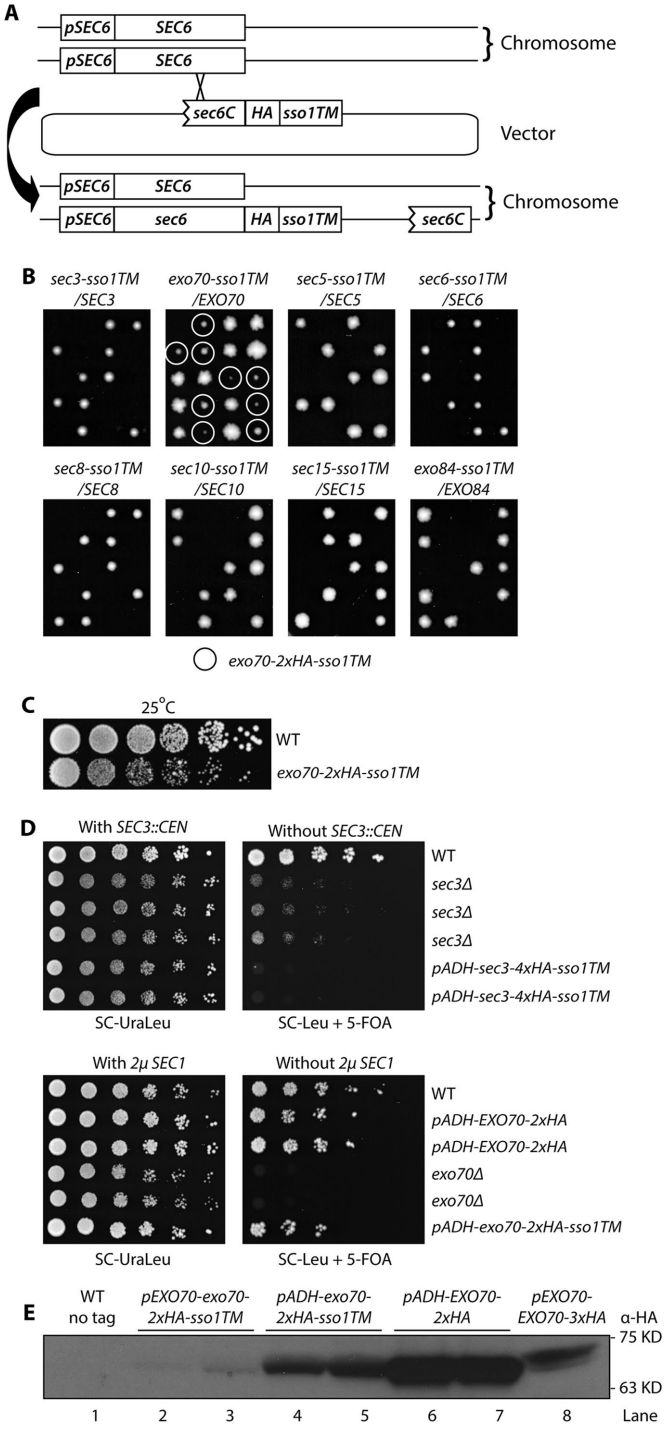

FIGURE 3: Exo70p is the only exocyst subunit that can function when anchored to the membrane through a C-terminal transmembrane (TM) domain. (A) The Sso1TM sequence was integrated at the C-terminal end of each exocyst subunit in one of the chromosomal copies in a WT diploid yeast strain. (B) The resulting diploid strains as indicated (NY3251, NY3253-3259) were sporulated and tetrads were dissected onto YPD plates, which were then incubated for 4 d at 25°C. The only viable mutant spores, *exo70-2xHA-sso1TM*, are marked with circles. (C) WT and *exo70-2xHA-sso1TM* strains (NY1210 and NY3260) were grown to early log phase in YPD medium at 25°C, serially diluted, spotted onto a YPD plate, and then incubated for 2 d at 25°C. (D) Top panel: WT, *sec3*Δ, and *pADH-sec3-4xHA-sso1TM* yeast strains with a complementing *SEC3* CEN URA vector (NY3263, 3262, and 3261) were grown to early log phase in SC-UraLeu liquid medium at 25°C, serially diluted, and spotted onto SC-Ura Leu or SC-Leu with 5′-FOA to select against the *SEC3* CEN plasmid. The plates were then incubated for 4–5 d at 25°C; bottom panel: WT, *pADH-EXO70-2xHA, exo70*Δ, and *pADH-exo70-2xHA-sso1TM* yeast strains carrying a bypass suppressor, 2μ *SEC1* URA3 plasmid (NY3267, 3266, 3265, and 3264) were analyzed as described above regarding the top panel. (E) Yeast strains as indicated (NY1210, NY3260, NY3268, NY3269, NY3241) were lysed quickly with NaOH (*Materials and Methods*). Tagged proteins were detected with anti-HA antibody.

We performed both invertase and Bgl2p secretion assays to analyze the efficiency of vesicular transport in the *exo70-TM* mutant strain. As shown in Supplemental Figure S2, *exo70-TM* cells accumulated a somewhat larger-than-normal internal pool of both invertase (13% vs. 1%) and Bgl2p (10% vs. 3% at 37°C), which is, however, relatively minor in comparison with *sec6-4*, a well-known exocyst mutant with a severe secretion defect. These data indicate that adding a transmembrane domain to the C-terminus of Exo70p does not seriously diminish its function. In summary, of the eight exocyst subunits, only Exo70p can function with a C-terminal TM domain.

To determine whether the exocyst subunits fused to the Sso1TM were actually anchored to the membrane, we performed fractionation by differential centrifugation. As shown in Figure 4A, a significant fraction of WT Exo70p, Sec3p, and Sec6p distributed to the 50,000 × *g* supernatant. However, all proteins bearing a C-terminal Sso1TM tail were almost completely excluded from the supernatant (Figure 4A, right panel), indicating that the TM tail had altered their subcellular distribution. Owing to the high quality of the anti-Sec10p and anti-Sec15p sera, we were able to use them to simultaneously detect both WT Sec10p or Sec15p and the alleles fused to Sso1TM in crude cell lysates of heterozygous diploid strains. This analysis clearly shows that the expression levels of WT and the corresponding allele anchored with a Sso1TM tail are similar and that the tail-anchored subunits are largely absent from the 50,000 × *g* supernatant, while the WT subunits were easily detected in this fraction (Figure 4B). We also compared the cellular distribution of overexpressed Exo70p-2xHA-Sso1TM (Figure 4C). As with all of the other tail-anchored exocyst subunits, it was absent from the supernatant. We noticed many degradation products in the lysate of cells overexpressing Exo70p-2xHA-Sso1TM (Figure 4C, top right panel). However, a more rapid lysis method did not yield these degradation products (Figure 3E, lane 4 and 5, and Supplemental Figure S3, lane 7), indicating that degradation had occurred predominantly after lysis. Therefore it appears that the subunits with a TM tail are largely intact in vivo and are stably anchored to the membrane.

The seven nonfunctional tail-anchored subunits might be inactive due to retention within the ER. Localization by immunofluorescence microscopy was not possible because the tags were not detected at their position between the open reading frame and the membrane anchor. However, subcellular fractionation by differential centrifugation (Supplemental Figure S6) demonstrated that tail anchored Sec3p, Sec10p, Sec15p, and Sec8p were predominantly in the 3000 × *g* supernatant, like the plasma membrane marker Sso1/2p and unlike the ER marker Sec61p. Tail anchored Sec5p and Exo84p were split between the supernatant and pellet, while only tail anchored Sec6p was predominantly in the pellet, like Sec61p. After normalizing for the distribution of Sso1/2p, all Sso1TM-anchored subunits except Sec6-Sso1TM showed a predominant cofractionation with the plasma membrane (Supplemental Figure S6). Thus, it appears unlikely that the failure of these constructs to function is due to a failure to exit the ER.

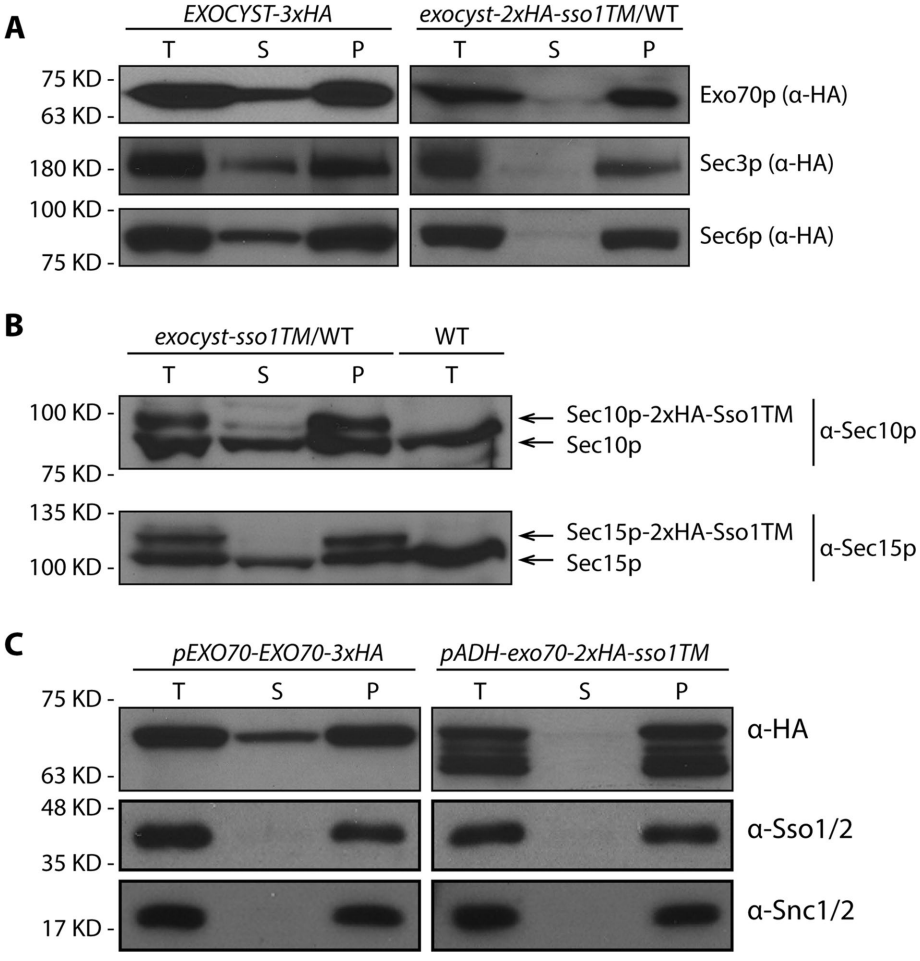

FIGURE 4: Exocyst subunits with a carboxy terminal TM tail were largely absent from the 50,000 × *g* supernatant. (A) Total cell lysates (T) from WT strains expressing *3xHA* or *2xHA-sso1TM* at the C-terminal end of *EXO70*, *SEC3*, or *SEC6* (NY3241, NY3252, NY3242, NY3253, NY3251, and NY3255) were centrifuged at 50,000 × *g*, separated into supernatant (S) and pellet (P) fractions, and analyzed by Western blot analysis on an 8% SDS–PAGE gel. Tagged proteins were detected with anti-HA antibody. Mutant strains are heterozygous diploids with one intact WT copy. (B) Total cell lysates (T), 50,000 × *g* supernatant (S) and pellet (P) fractions from heterozygous diploid strains, *SEC10-2xHA-sso1TM/WT* (NY3257) or *SEC15-2xHA-sso1TM/WT* (NY3258), were analyzed by Western blot with anti-Sec10p or anti-Sec15p serum. Total lysate from WT (NY1210) was used as a control. (C) Total cell lysates (T), 50,000 × *g* supernatant (S), and pellet (P) fractions from *pEXO70-EXO70-3xHA* (NY3241) or *pADH-exo70-2xHA-sso1TM* (NY3268) were analyzed by Western blot with anti-HA antibody. Control membrane protein Sso1/2p was detected with anti-Sso1/2 and Snc1/2p was detected with anti-Snc1/2 sera.

In summary, Exo70p is the only subunit that can function when anchored to the membrane through a C-terminal transmembrane (TM) domain. Higher levels of expression improved cell growth somewhat. These findings imply that Exo70p can perform its function at the membrane and that the cytosolic pool is not essential.

Endocytosis is dispensable for the viability of the *TM-sec3* or *exo70-TM* strains

Sec3p is the only exocyst subunit that can function well when anchored to the membrane at its N-terminus, while Exo70p is the only one that can function when anchored at its C-terminus. These results suggest that Sec3p and Exo70p function exclusively on the membrane, presumably the plasma membrane, rather than in the cytosol. Nonetheless, endocytosis could be utilized by *TM-sec3* or *exo70-TM* expressing cells to recycle them from the plasma membrane, through endosomes and the Golgi so that they could act on secretory vesicles. To test this possibility, we examined the viability of *TM-sec3* or *exo70-TM* yeast strains in which endocytosis had been compromised. To simplify the analysis, we selected two gene deletions that inhibit endocytosis at different stages yet exhibit no obvious growth defect of their own. Syp1p is an endocytic adaptor protein that arrives early at endocytic sites and functions in endocytic site turnover and placement (Stimpson *et al.*, 2009; Apel *et al.*, 2017). Tlg2p is a t-SNARE that mediates fusion of endosome-derived vesicles with the late Golgi (Abeliovich *et al.*, 1998; Lewis *et al.*, 2000). The *tos2TM-sec3* and *exo70-sso1TM* yeast strains were crossed with *syp1*Δ and *tlg2*Δ strains and double mutants were isolated by tetrad dissection. We then performed growth tests to compare the effects of *TM-sec3* or *exo70-TM* on growth in a WT background relative to the *syp1*Δ or *tlg2*Δ strain backgrounds (Figure 5 and Table 1). We found that *syp1*Δ did not exhibit any synthetic growth effects in combination with *tos2TM-sec3-4xHA* (Figure 5A, compare rows 3 and 4), *exo70-2xHA-sso1TM* (Figure 5C, compare row 1 and 3), or *exo70-2xHA-sso1TM* expressed from the *ADH1* promoter (Figure 5E, compare rows 1 and 2). In the case of crosses to *tlg2*Δ, we observed relatively mild synthetic effects in several situations, for example, *tos2TM-sec3-4xHA tlg2*Δ double mutants are slow growing at 37°C (Figure 5B, right panel, compare rows 3 and 4). Another exception is that when *exo70-2xHA-sso1TM* was overexpressed, it showed a mild synthetic negative effect with *tlg2*Δ at 25°C, 30°C, and 34°C and a stronger effect at 37°C (Figure 5F, compare rows 1 and 2). Endocytosis can be used by membrane proteins to maintain their polarity, countering the effects of diffusion, which would otherwise allow membrane proteins to move away from their site of insertion. Therefore, endocytosis can be an important contributory mechanism, even for a protein that functions exclusively at the plasma membrane, such as Sso1p (Valdez-Taubas and Pelham, 2003). However, if a protein also functions on secretory vesicles or the cytosol and requires rapid recycling from the plasma membrane, the addition of a transmembrane domain in combination with a partial endocytic block would be expected to cause a severe loss of function. The weak or negligible genetic interactions observed between *TM-sec3* or *exo70-TM* and *syp1*Δ or *tlg2*Δ suggest that Sec3p and Exo70p function predominantly at the plasma membrane. Syp1p functions at a very early step of endocytosis and is an adaptor only for a subset of cargo proteins (Stimpson *et al.*, 2009; Apel *et al.*, 2017). Deletion of *SYP1* causes defects in the lifetime of endocytic sites, but does not prevent their internalization, whereas deletion of *TLG2* has a more severe effect on endocytosis, blocking vesicular traffic from the endosome to the late Golgi (Abeliovich *et al.*, 1998).

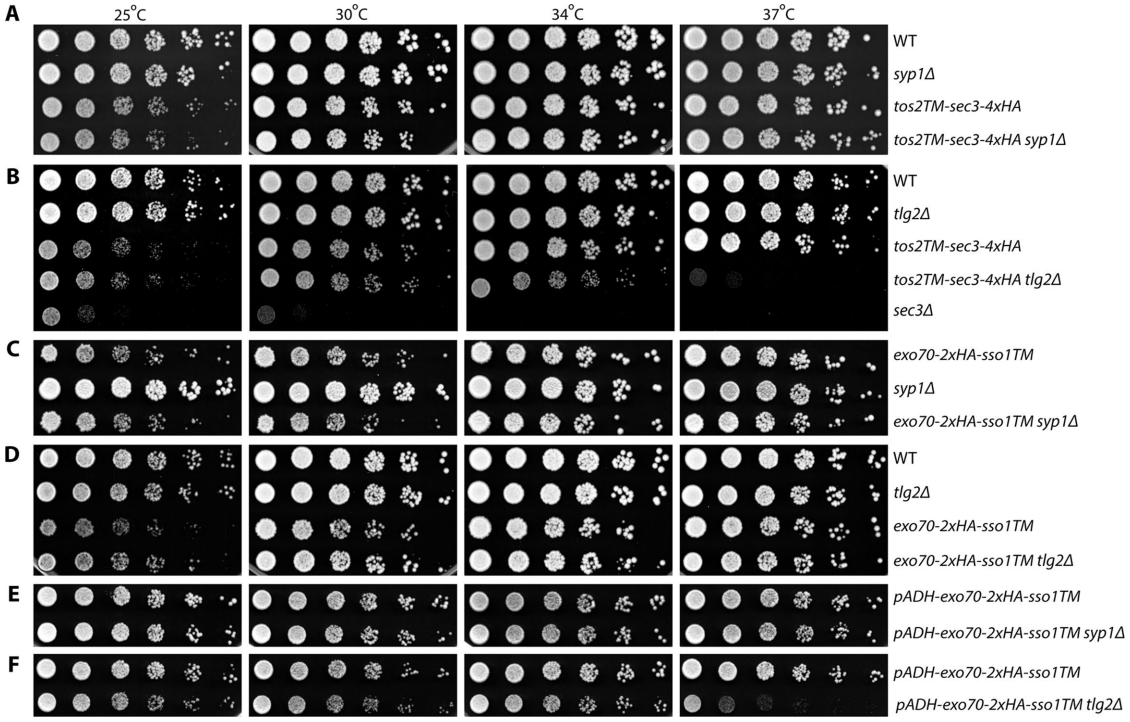

FIGURE 5: Endocytosis is dispensable for the viability of *TM-sec3* or *exo70-TM* yeast stains. (A–F) Strains as indicated were grown to early log phase in SC medium at 25°C, serially diluted, and spotted on SC plates. The plates were then incubated for 2 d at 25°C, 30°C, 34°C, and 37°C, respectively.

TM-anchored Exo70p reduces the cytosolic pool of the other exocyst subunits, but TM-anchored Sec3p does not

The viability of *tos2TM-sec3* and *exo70-sso1TM* strains in both a WT background and in endocytosis-deficient backgrounds suggests that Sec3p and Exo70p can function exclusively at the plasma membrane. Next we examined the subcellular distribution of the other exocyst subunits in these cells in which Sec3p or Exo70p were stably anchored to the membrane through TM domains. By taking advantage of the high quality of anti-Sec10p and anti-Sec15p sera, we were able to examine the distribution of untagged Sec10p and Sec15p in *TM-sec3* or *exo70-TM* yeast lysates. We performed fractionation by differential centrifugation and found that, in addition to the loss of Exo70p-2xHA-sso1TM from the 50,000 × *g* supernatant (Figure 4C), Sec10p and Sec15p were also depleted from this supernatant (Figure 6A, lane 2). This suggests that the linkage between Exo70p and these other exocyst subunits is robust. However, the linkage with Sec3p appeared to be weaker, as the cellular distribution of Sec10p and Sec15p was normal when Sec3p was stably anchored to the membrane through an N-terminal TM anchor (Figure 6A, compare lanes 5 and 8).

To gain a more complete understanding of the subcellular distribution and assembly state of the exocyst subunits in *TM-sec3* or *exo70-TM* yeast strains, we added a FLAG tag to another exocyst subunit and then performed a FLAG-IP to purify the tagged subunit together with all associated proteins from the 50,000 × *g* supernatant (Figure 6B). The immunoprecipitation efficiency is ~30–50% (Supplemental Figure S7). The supernatant would potentially include any free soluble monomers, a fully assembled exocyst complex, and subcomplexes; however, membrane-associated proteins or protein complexes should be largely excluded since no detergent was added prior to centrifugation. The level of each of the exocyst subunits was determined by Western blotting with all available anti-exocyst sera or anti-FLAG antibody. To simplify the comparison between WT lysate and lysates expressing a TM-anchored subunit, we adjusted the loading to have an equal amount of the FLAG-tagged subunit and then compared the level of all of the other subunits. When we precipitated Sec8p-3xFLAG from the supernatant of an *exo70p-sso1TM* lysate, we found that the relative amounts of four of the exocyst subunits (Exo70p-Sso1TM, Sec3p, Sec15p, and Exo84p) were dramatically decreased relative to WT. Sec10p was partially reduced, and Sec6p was the least affected, consistent with the notion that Sec6p and Sec8p are closely associated (Figure 6B, compare lanes 1 and 2). Furthermore, the absolute amount of exocyst subunits present in the *exo70-sso1TM* supernatant was low relative to WT since we had to load twice as much to detect a similar amount of Sec8p-3xFLAG in the precipitate. We also precipitated another FLAG-tagged exocyst subunit, Sec5p, from the *exo70-sso1TM* supernatant. To detect a similar amount of Sec5p-3xFLAG, we had to load almost four times as much of the precipitate for *exo70-sso1TM* as for WT. We observed that under this condition, all exocyst subunits, except for Exo70p-Sso1TM itself, showed a normal relative abundance in WT and the Exo70p-Sso1TM supernatant (Figure 6B, compare lanes 3 and 4). Together, these two sets of data suggest that the association between Exo70p and the other exocyst subunits is strong. When Exo70p is stably anchored, substantial fractions of the other subunits are also depleted from the cytosol.

Mutants	*syp1*Δ	*tlg2*Δ
tos2TM-sec3-4xHA	No effect	Synthetically sick at 37°C
exo70-2xHA-sso1TM	No effect	No effect
pADH-exo70-2xHA-sso1TM	No effect	Synthetically sick, mildly at 25–34°C, strongly at 37°C

TABLE 1: Summary of genetic interactions between *sec3* or *exo70* mutants and *syp1*Δ or *tlg2*Δ.

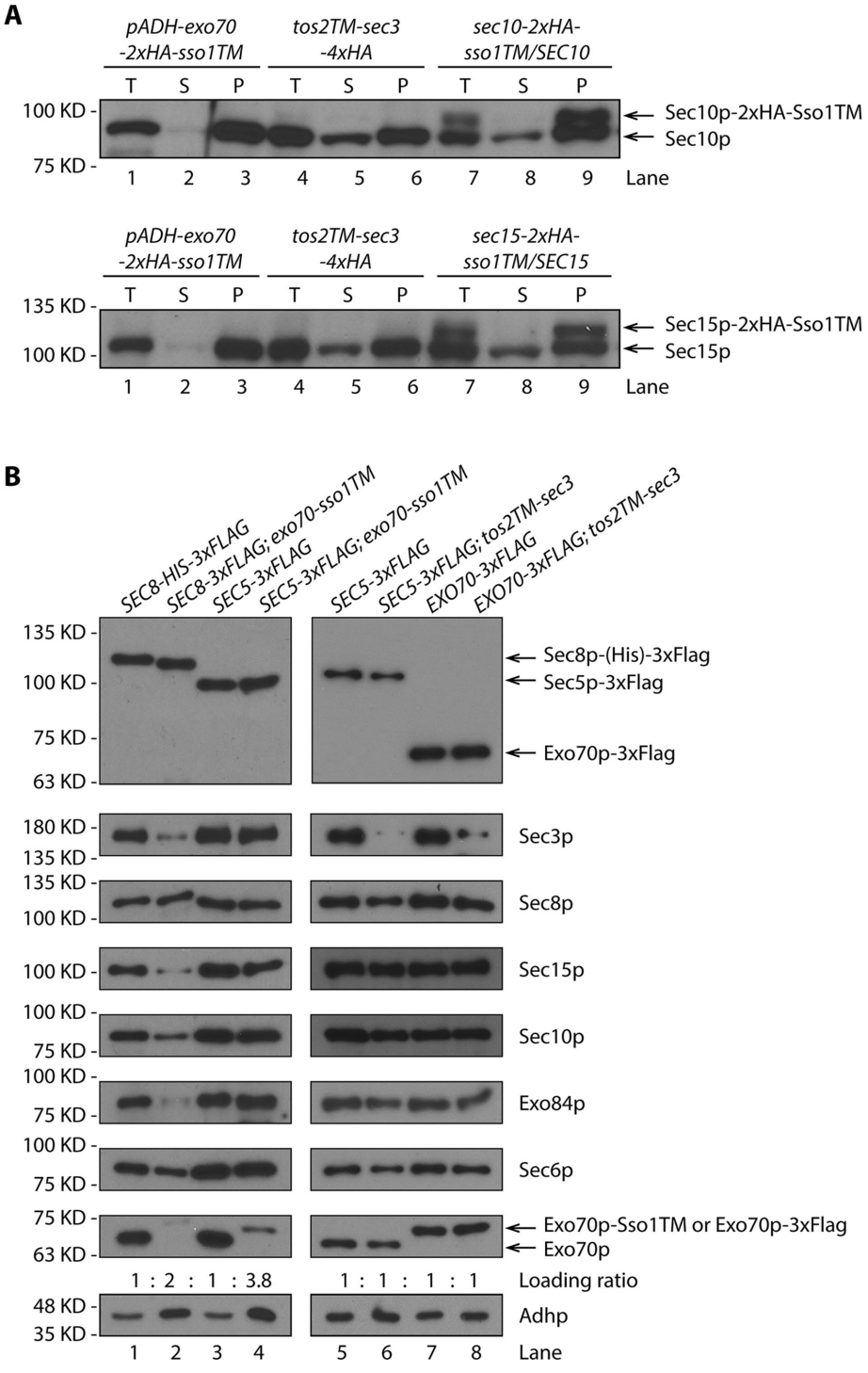

FIGURE 6: The cellular distribution of exocyst subunits when Exo70p or Sec3p are irreversibly anchored to the membrane. (A) Total cell lysates (T) and 50,000 × *g* supernatant (S) and pellet (P) fractions from *exo70-sso1TM* and tos2*TM-sec3* (NY3268 and NY3238) were analyzed by Western blot with anti-Sec10p or anti-Sec15p serum. Heterozygous *sec10-sso1TM* diploid strain (NY3257, top panel) and *sec15-sso1TM* diploid strain (NY3258, bottom panel) were used as control. Proteins were detected with anti-Sec10p (top panel) or anti-Sec15p (bottom panel) serum. (B) Yeast strains as indicated (left panel: NY3271, NY3275, NY3276, and NY3277; right panel: NY3276, NY3278, NY3279, and NY3280) were lysed and the 50,000 × *g* supernatant was used in precipitations with anti-Flag beads. Eluted proteins were detected with anti-Flag, anti-Sec3p, anti-Sec8p, anti-Sec15p, anti-Sec10p, anti-Exo84p, anti-Sec6p, and anti-Exo70p antibodies. Loading was normalized to have an approximately equal amount of the FLAG-tagged subunit, and then the level of all of the other subunits was compared. The relative loading for each sample is listed. Using the same loading ratio, Adhp levels in the 50,000 × *g* supernatants were examined to reflect the differences in loading.

When we immunoisolated Sec5p-3xFLAG or Exo70p-3xFLAG from *TM-sec3* supernatants, the results were quite different. Other than TM-Sec3p itself, all subunits showed similar abundance in the precipitates derived from the WT and *TM-sec3* supernatants, regardless of which subunit was tagged (Figure 6B, compare lanes 5 and 6 and lanes 7 and 8) and no adjustment to the loading was needed. Therefore, even though Sec3p was stably anchored to the membrane, the distribution of the other subunits between the membrane and cytosol was unaffected and the cytosolic pools assembled well without Sec3p. This suggests that the association between Sec3p and the other subunits is relatively loose. Taken together, our data suggest that Exo70p and Sec3p can function when stably bound to the plasma membrane. The other subunits associate with them; however, the association with Exo70p is tighter than with Sec3p.

Additional exocyst subunits are recruited to the cell cortex when either Exo70p or Sec3p is membrane anchored

When either Exo70p or Sec3p was anchored to the membrane with a transmembrane domain, differential centrifugation fractionation experiments showed that they were nearly absent from the 50,000 × *g* supernatant, suggesting a stable association with the membrane. To examine their subcellular localization in vivo, we added a GFP tag to the N-terminus of Exo70p-2xHA-Sso1TM and to the C-terminus of Tos2TM-Sec3p-4xHA since detection by immunofluorescence was less sensitive. These constructs conferred the same growth properties as those lacking the GFP tag (Supplemental Figure S8). As shown in Figure 7A, in contrast to the typical bud tip or bud neck localization of WT Exo70p-GFP (top panels 1 and 2), GFP-Exo70p-2xHA-Sso1TM showed a fairly uniform distribution along the entire cell periphery (top panels 3 and 4), similarly to that of Sso1p (Brennwald *et al.*, 1994; Valdez-Taubas and Pelham, 2003). A minor fraction of the GFP-fluorescence was observed on internal structures that colocalized with the fluorescent dye FM4-64 marking the vacuole (Supplemental Figure S9). Several other exocyst subunits, including Sec5p, Sec8p, and Exo84p, also localized to the cell periphery in cells expressing Exo70p-2xHA-Sso1TM (Figure 7B, columns 3 and 4), consistent with the finding from FLAG IP experiments that when Exo70p is membrane anchored, other subunits are also depleted from the

cytosol (Figure 6). Membrane-anchored Tos2TM-Sec3p-4xHA-GFP, localized to the cell periphery, in addition to bud tips and bud necks (Figure 7A, bottom panels 3 and 4). Intriguingly, although FLAG IP data suggest a relatively loose association between Sec3p and the other exocyst subunits in lysates (Figure 6), in vivo, Sec5p-GFP, Sec8p-GFP, and Exo84p-GFP display some relocalization to the cell periphery in response to Tos2TM-Sec3p-4xHA expression (Figure 7B, columns 5 and 6). It is possible that, in vivo, the other subunits are bound to Tos2TM-Sec3p-4xHA; however, after lysis, they dissociate and can therefore be found in the cytosol fraction.

Sec3p is unstable in *act1-3* lysates

Several studies have found that the localization of Sec3p to sites of polarized surface growth is at least partially resistant to the disruption of actin cables, while the localization of the other exocyst subunits is predominantly actin dependent (Finger *et al.*, 1998; Boyd *et al.*, 2004). This has led to a proposal that Sec3p can be recruited directly to these sites by binding to cortical polarity determinants, while the other subunits are delivered to these sites by riding on secretory vesicles as they are actively transported along actin cables by the Myo2p motor. To reveal the effects of the loss of actin function on exocyst assembly, we isolated the complex from a temperature-sensitive actin mutant, *act1-3*. We used FLAG tags to immunoisolate the complex from lysates that had been generated by grinding flash-frozen yeast under liquid nitrogen, conditions that have been shown to stabilize the complex (Heider *et al.*, 2016). At the permissive temperature, 20°C, both WT and *act1-3* cells expressing Sec8p-His-3xFlag yielded a complex containing all eight subunits in approximately equal stoichiometry (Figure 8A, left panel). Following a 2 h shift from the permissive temperature, 20°C, to 37°C, WT cells yielded the same set of exocyst subunits and in a similar amount. In contrast, *act1-3* cells yielded a complex in which Sec3p was

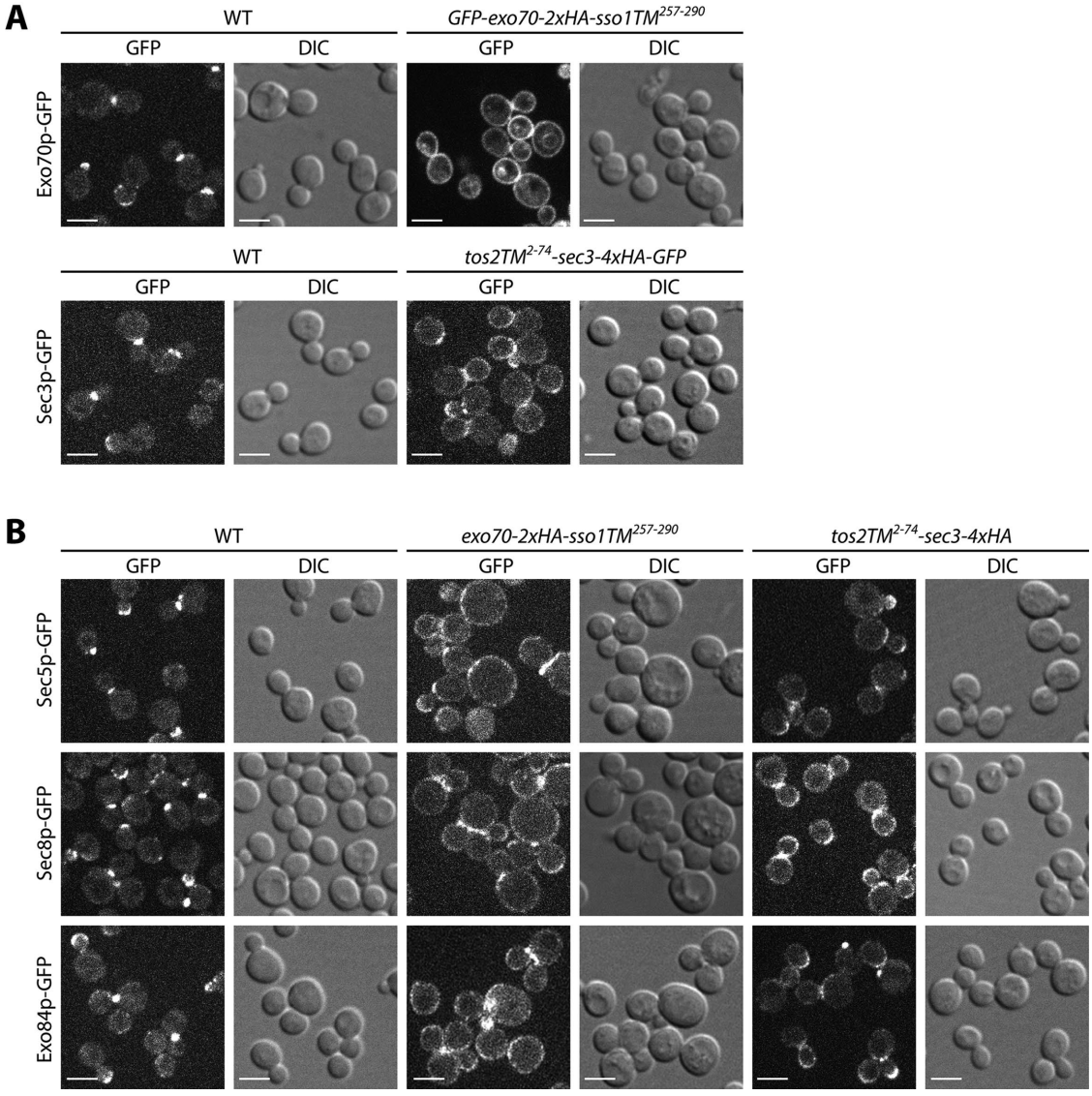

FIGURE 7: Localization of exocyst subunits in membrane anchored Exo70p or Sec3p strains. (A) A GFP tag was added to Exo70p or Sec3p in WT and TM anchored *EXO70* or *SEC3* strains. Yeast cells were grown to early log phase in selection medium at 25°C and harvested, and the live cells were directly examined by fluorescence microscopy. Bars, 5 µm. (B) A GFP tag was added to Sec5p, Sec8p, or Exo84p in WT and TM-anchored *EXO70* or *SEC3* strains. Yeast cells were grown to early log phase in selection medium at 25°C and harvested, and the live cells were directly examined by fluorescence microscopy. Bars, 5 µm.

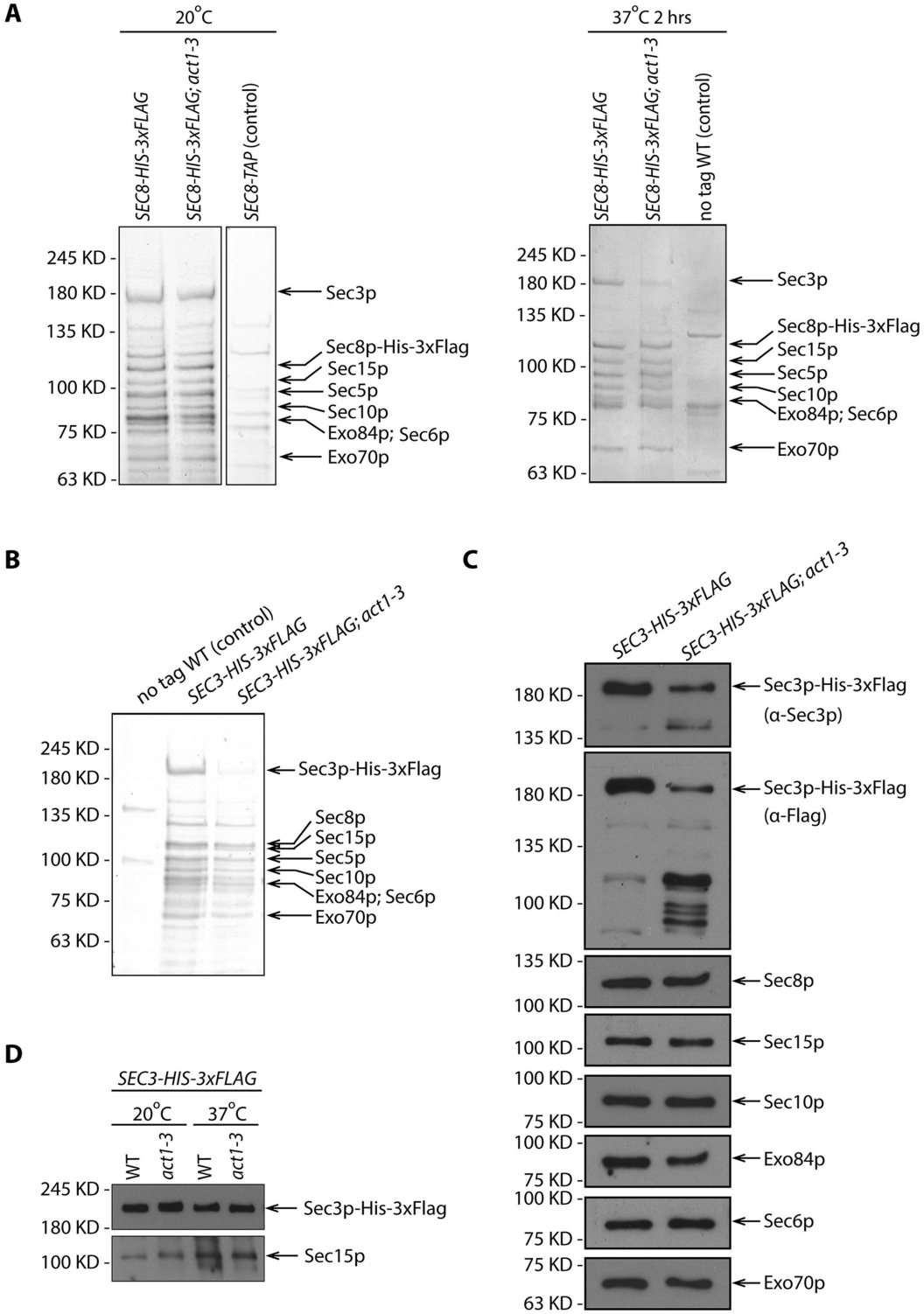

FIGURE 8: Sec3p is unstable in *act1-3* lysate. (A) SDS–PAGE and Coomassie staining of exocyst complexes purified using Sec8p-His-3xFlag from WT and *act1-3* mutant yeast lysates (NY3271 and NY3272). Left panel shows the purification from yeast strains growing at permissive temperature 20°C. Right panel shows the purification from yeast strains shifted to nonpermissive temperature 37°C for 2 h before harvesting. WT strains with Sec8p-TAP tagged or Sec8p untagged were used as negative controls respectively. For comparison, the loading ratio for the purified samples from WT and *act1-3* is 1:1. (B) SDS–PAGE and Coomassie staining of exocyst complexes purified with Sec3p-His-3xFlag from WT and *act1-3* mutant yeast strains (NY3273 and NY3274). For comparison, the loading ratio for the purified samples from WT and *act1-3* is 1:2. (C) Western blot analysis of immunoisolated exocyst with Sec3p-His-3xFlag from WT and *act1-3* mutant yeast strains (NY3273 and NY3274) on a 6% SDS–PAGE gel. Proteins were detected with anti-Flag, anti-Sec3p, anti-Sec8p, anti-Sec15p, anti-Sec10p, anti-Exo84p, anti-Sec6p, and anti-Exo70p antibodies. For comparison, the loading ratio for the purified samples from WT and *act1-3* is 1:2. (D) Total cell lysates by quick NaOH lysis from WT and *act1-3* mutant yeast strains were analyzed by Western blot with anti-Flag antibody and anti-Sec15p serum.

significantly underrepresented relative to the other subunits (Figure 8A, right panel). To determine whether Sec3p was present as a monomer, independent of the exocyst, or in some alternate complexes, we isolated Sec3p-His-3xFlag from WT and *act1-3* cells. Although the amount of the exocyst complex isolated from *act1-3* cells was dramatically reduced since we had to load twice as much to detect a similar amount of most exocyst subunits, it appeared to consist of the same components as in WT cells (Figure 8, B and C). However, the yield of Sec3p-His-3xFlag itself from *act1-3* lysates was further reduced relative to the other seven subunits. This finding prompted us to question whether the apparent loss of Sec3p-His-3xFlag occurred in vivo or during the immunoisolation protocol. A rapid alkaline lysis method revealed a similar ratio between full-length Sec3p-His-3xFlag and Sec15p in *act1-3* and WT samples at both 20° and 37°C (Figure 8D). Thus we deduce that the loss of Sec3p-His-3xFlag in *act1-3* samples must take place during the immuno-isolation procedure. This suggests that either the proteolytic activity is increased in *act1-3* lysates relative to WT or that Sec3p-His-3xFlag is more accessible to proteases in *act1-3* lysates. In either case, the effects are limited to Sec3p as the other subunits were unaffected.

DISCUSSION

We have shown that Sec3p and Exo70p are unique among the exocyst subunits as they alone can function well when irreversibly anchored to the plasma membrane by a transmembrane domain. To preserve functionality, Sec3p must be anchored at its N-terminus, while Exo70p must be anchored at its C-terminus. A structure of the assembled exocyst has been recently proposed based on trilateration using end-to-end dimensional measurements made by light microscopy (Picco *et al.*, 2017). We can now orient the proposed structure relative to the plasma membrane with both the N-terminus of Sec3p and the C-terminus of Exo70p facing toward the plasma membrane (Supplemental Figure S10). This orientation also allows the N-terminus of Exo84p to face the plasma membrane, consistent with our observation that *tos2TM-exo84* cells are viable, albeit just barely. The orientation agrees well with studies showing that both the N-terminus of Sec3p and the C-terminus of Exo70p can bind to $PI(4,5)P_2$, a lipid predominantly associated with the cytoplasmic leaflet of the plasma membrane (He *et al.*, 2007; Zhang *et al.*, 2008). This orientation would also permit Sec3p and Exo70p to interact with cortical polarity determinants Cdc42p, Rho1p, Rho3p, and Bem1p (Guo *et al.*, 2001; Zhang *et al.*, 2001; Liu and Novick, 2014).

The ability of Tos2TM-Sec3p and Exo70p-Sso1TM to function without any significant cytosolic pool indicates that their essential functions can be fulfilled exclusively on the membrane. Furthermore, the absence of any strong synthetic effect in combination with endocytic mutants suggests that these subunits do not need to recycle from the plasma membrane onto secretory vesicles. These observations are consistent with the proposal that Sec3p and Exo70p serve to mark specialized exocytic sites on the plasma membrane (Finger *et al.*, 1998; Boyd *et al.*, 2004).

Whether or not the other six exocyst subunits can also act exclusively on the plasma membrane is not yet clear. Although they are nonfunctional when directly anchored to the membrane, this could reflect an inappropriate orientation rather than a requirement for a cytosolic pool. Immunofluorescence microscopy and fractionation by differential centrifugation suggest that the nonfunctional constructs are, with the exception of Sec6-Sso1TM, delivered to the plasma membrane with an efficiency of at least 50%. In the case of Sec6p, the proposed orientation does place the N-terminus near the membrane (Supplemental Figure S10); nonetheless, Tos2TM-Sec6p-expressing cells were found to be inviable. Hence, it is plausible that the cytosolic pool of Sec6p, unlike that of Sec3p or Exo70p, plays an essential function. In *tos2TM-sec3* cells, the remaining seven subunits can still be found at normal levels in the cytosolic fraction within an assembled complex, while in *exo70-sso1TM* cells the other subunits are depleted from the cytosol, yet are still present at about one quarter to one half of their normal levels. Thus, our data are consistent with an essential role for the cytosolic pools of these subunits, perhaps in recycling from the cell cortex onto newly formed secretory vesicles, yet other explanations could also account for these observations.

To address the possibility of an assembly cycle, we have examined the composition of the exocyst in *act1-3* cells. This mutant is blocked in the active delivery of secretory vesicles to the polarized exocytic sites typically marked by Sec3p, although vesicles continue to fuse with the plasma membrane in a depolarized manner with a kinetic delay (Novick and Botstein, 1985). The observed loss of Sec3p from the isolated complex in *act1-3* cells is consistent with a cycle in which Sec3p normally joins the complex as vesicles arrive at exocytic sites and then dissociates following vesicle fusion. Nonetheless, our inability to isolate a free, unassembled pool of Sec3p from *act1-3* lysates leaves the issue unresolved. Sec3p is present at normal levels relative to other exocyst subunits in *act1-3* cells, yet is apparently degraded after lysis during affinity purification. The heightened sensitivity of Sec3p to degradation in *act1-3* lysates could reflect an increase in its accessibility to proteases due to a failure in exocyst assembly. While we cannot exclude an alternate possibility in which proteolytic activity is increased in *act1-3* lysates, none of the other subunits were similarly affected.

In total, our findings help orient the exocyst complex with respect to the membrane and provide important clues regarding the site of action of its various components.

MATERIALS AND METHODS

Plasmid and yeast strain construction

The plasmids and yeast strains used in this study are listed in Supplemental Tables S1 and S2. To generate a Sec3 CEN yeast expression vector, pRS316-Sec3 (NRB1623), full-length *SEC3*, including its 231–base pair 5′UTR and 488–base pair 3′UTR, was PCR amplified from WT yeast genomic DNA and inserted into *Bam*HI-*Kpn*I linearized pRS316 by gap repair. To generate the HemiZap vector, pRS305-pSec3-Tos$2^{2\text{-}74}$-Sec3-4xHA-Adh1t (NRB1624), Sec3 5′ UTR 772 base pairs, Tos2 ORF for amino acids 2–74, and Sec3-4xHA were sequentially PCR amplified from WT or NY2128 yeast genomic DNA and cloned into *Xho*I-*Bam*HI linearized pRS305-Adh1t. To add GFP to the C-terminal end of the above construct (NRB1650), GFP was PCR amplified, digested with *Bgl*II/*Bam*HI, and inserted into *Bgl*II/*Bam*HI linearized pRS305-pSec3-Tos$2^{2\text{-}74}$-Sec3-4xHA-Adh1t. To generate pRS305-pExo70-Tos$2^{2\text{-}74}$-Exo70-3xHA-Adh1t (NRB1625), Exo70 5′ UTR 1180 base pairs, Tos2 ORF for amino acids 2–74, and Exo70-3xHA were sequentially PCR amplified from WT or NY3241 yeast genomic DNA and cloned into *Xho*I-*Sac*II linearized pRS305-Adh1t.

To construct a yeast strain with a transmembrane (TM) domain at the N-terminus of Sec3 (NY3237), a HemiZAP vector (NRB1624) was transformed into the *SEC3* promoter region in a *sec3*Δ yeast strain that was complemented with a *SEC3* expression CEN vector carrying the *URA3* marker (NY3236). After spotting on a 5′-FOA plate, the complementing CEN vector was removed, resulting in a single copy of *SEC3* fused to the N-terminal TM domain from Tos2 (NY3238). A similar method was used to generate a yeast strain expressing Tos$2^{2\text{-}74}$-Exo70-3xHA (NY3240).

To generate pRS306-pSec6-Tos2$^{2-74}$-Sec6N (NRB1626), the Sec6 5′ UTR 999 base pairs, Tos2 ORF for amino acids 2–74, and Sec6 N-terminal 678 base pairs were sequentially PCR amplified from WT yeast genomic DNA and cloned into *Xho*I-*Sac*II linearized pRS306-Adh1t. Similar approaches were used to generate Exo84, Sec8, Sec10, Sec15, and Sec5 HemiZAP constructs (NRB1627-1631).

To construct a yeast strain with a TM domain at the N-terminus of Sec6, a Sec6 C-terminal HA-tagged yeast strain (NY3242) was first mated with a WT strain to generate a diploid, which was then transformed with the integration vector described above (NRB1626). Transformants in which integration had occurred in the tagged chromosome were selected by PCR. These transformants have one WT copy of *SEC6* and another copy of *sec6* with an N-terminal TM domain from *TOS2* (NY3243). After sporulation and tetrad dissection, a spore was selected that carried only one copy of *sec6* with an N-terminal *tos2TM* anchor. Similarly, N-terminal *tos2TM* anchored *EXO84*, *SEC8*, *SEC10*, *SEC15*, and *SEC5* yeast strains were generated (NY3245-3248, NY3250).

To construct yeast strains with a TM domain at the C-terminal end of the exocyst subunits, a set of HemiZAP integration vectors (NRB1633–1640) were first generated. For example, to create pRS305-Exo70-2xHA-Sso1TM$^{257-290}$ (NRB1633), the Sso1 C-terminal 34 codons (257–290) were PCR amplified from WT genomic DNA with *Bam*HI and *Xba*I sites on either side. It was then double digested with *Bam*HI/*Xba*I and inserted into pRS305-Exo70-3xHA (NRB1632) linearized with the same two enzymes. Similar approaches were used to generate Sec6, Sec15, Exo84, Sec10, Sec5, Sec8, and Sec3 HemiZAP constructs (NRB1634–1640). These HemiZAP vectors were then linearized with a unique enzyme (see Supplemental Table S1) and transformed into a WT diploid yeast strain (NY2696) to integrate into one WT copy of the gene locus. The other copy was kept as WT (NY3251, 3253-3259). PCR-verified diploid transformants, which have one WT copy and one copy with a C-terminal Sso1TM tail, were sporulated and dissected to isolate a haploid with only one copy of the gene, which has the Sso1TM tail.

To generate the overexpression CEN vector p415ADH-Sec3-4xHA-Sso1TM$^{257-290}$ (NRB1641), Sec3-4xHA and Sso1TM$^{257-290}$ were sequentially PCR amplified using NY2128 genomic DNA as template and cloned into the p415ADH (NRB867) *Bam*HI/*Xho*I site. To generate the overexpression CEN vector p415ADH-Exo70-2xHA-Sso1TM$^{257-290}$ (NRB1642), Exo70-2xHA-Sso1TM$^{257-290}$ was PCR amplified from NY3260 genomic DNA with *Xba*I and *Pst*I sites on either side and cloned into the p415ADH (NRB867) *Xba*I/*Pst*I site. To add GFP to the N-terminal end of Exo70 (NRB1649), GFP was PCR amplified, digested with *Xba*I, and inserted into *Xba*I-linearized p415ADH-Exo70-2xHA-Sso1TM$^{257-290}$. The corresponding WT construct p415ADH-Exo70-2xHA (NRB1643) was generated by introducing a stop codon after the 2xHA sequence by site-directed mutagenesis. These CEN vectors were transformed into *sec3*Δ or *exo70*Δ yeast strains that were balanced by *SEC3*::CEN (*URA3*) or *SEC1*::2μ (*URA3*), respectively (NY3261, 3264). The balancing constructs were then removed by growth on 5′-FOA to generate C-terminal TM anchored Sec3 or Exo70 overexpression yeast strains.

To construct HemiZAP vectors for adding a 3xFlag tag to the C-terminal end of exocyst subunits (NRB1646–1648), 909, 653, and 1637 nucleotides of the C-terminal end of Sec8, Sec5, and Exo70, respectively, were cloned into *Xho*I/*Xma*I sites in pRS306-3xFlag-Adh1t. For Sec3 and Sec8 (NRB1644–1645), 886 and 1569 nucleotides of the C-terminal end of Sec3 and Sec8 were cloned into *Xho*I/*Not*I or *Bam*HI/*Not*I sites in pRS305-His-3xFlag-Adh1t.

The *syp1*Δ *and tlg2*Δ yeast deletion strains (NY3290-3291) were generated by the method of Longtine *et al*. (1998).

Growth test

Yeast cells were grown overnight in yeast peptone dextrose (YPD) or synthetic complete (SC) dropout medium to stationary phase. Cells were washed once with sterile water and diluted to an OD_{600} of 0.5. Cells were spotted in fivefold serial dilutions starting with an OD_{600} of 0.5 onto YPD, SC dropout, or SC with 5′-FOA plates. Plates were incubated at the indicated temperature for 2 to 4 d.

Rapid protein extraction from yeast

Yeast cells were grown to OD_{600} ~ 1 at 25°C, and 2.5 OD_{600} units of cells were harvested. Cell pellets were resuspended in 100 μl of water and then mixed with 100 μl of 0.2 M NaOH. After 5 min incubation at room temperature (RT), cells were pelleted, resuspended in 50 μl of 1 × SDS sample buffer, and boiled for 3 min (Kushnirov, 2000). Proteins were subjected to Western blot analysis with mouse monoclonal anti-HA antibody (Covance; HA.11 clone 16B12) at 1:1000 dilution or mouse monoclonal anti-Flag antibody (Sigma; F3165) at 1:2000 dilution.

Low-speed fractionation

Low-speed fractionation was performed to separate ER and plasma membrane-associated proteins (Ruohola and Ferro-Novick, 1987; Walworth and Novick, 1987). Yeast cells were grown at 25°C to mid–log phase in YPD medium. About 100 OD_{600} cells were harvested by centrifugation at 1500 × *g* for 10 min. Pellets were washed once with 10 mM NaN_3 and then resuspensed in 5 ml of spheroplast medium (1.4 M sorbitol, 50 mM KPi, pH 7.5, 10 mM NaN_3, 56 mM β-mercaptoethanol, zymolyase 0.2 mg/ml). After incubation at 37°C in a water bath with gentle shaking for 30 min, the spheroplast mixture was layered onto 10 ml of sorbitol cushion (1.7 M sorbitol, 20 mM KPi, pH 7.5) and centrifuged for 10 min at 1500 × *g*. The spheroplasts were resuspended in 1.2 ml lysis buffer (0.8 M sorbitol, 10 mM triethanolamine, pH 7.2, 1 mM EDTA, 10 mM NaN_3, 1 mM phenylmethanesulfonyl fluoride [PMSF], 2× protease inhibitor cocktail), homogenized 10 times using a 1-ml Wheaton tissue grinder, and then centrifuged at 500 × *g* for 3 min to remove unbroken cells. An aliquot (75 μl) of supernatant was mixed with 75 μl of 2 × sample buffer (total fraction [T]) and heated at 100°C for 5 min. Of the remaining portion, 500 μl was centrifuged for 6 min at 3000 × *g* at 4°C. Of the supernatant (S), 75 μl was mixed with 75 μl of 2× sample buffer and heated at 100°C for 5 min. The pellet (P) was resuspended in 500 μl of lysis buffer, and 75 μl was mixed with 75 μl of 2× sample buffer and heated at 100°C for 5 min. Exocyst proteins were detected by SDS–PAGE followed by Western blotting with anti-HA mouse monoclonal antibody (Covance HA.11 clone 16B12 or Sigma H3663) or anti-myc mouse monoclonal antibody (9E10). Sso1/2p was detected with anti-Sso1/2 serum (1:5000; Novick lab collection). Sec61p was detected with anti-Sec61 serum (1:1000; kindly provided by Jeffrey L. Brodsky, University of Pittsburgh, Pittsburgh, PA).

High-speed fractionation

A total of 100 OD_{600} units of yeast cells were pelleted and resuspended in 1.2 ml of lysis buffer (10 mM Tris HCl, pH 7.4, 150 mM NaCl, 1 mM EDTA, 1 mM dithiothreitol (DTT), 1 mM PMSF, 2× protease inhibitor cocktail). The cell suspension was transferred into a 2-ml screw cap tube (Thermo Fisher Scientific) with 2 g zirconia/silica

0.5-mm beads (Biospec Products) that had been prewashed with ice-cold lysis buffer without protease inhibitor and shaken twice for 3 min with a 1-min interval. The lysate was centrifuged for 2 min at 500 × *g* at 4°C. An aliquot (75 µl) of supernatant was mixed with 75 µl of 2× sample buffer (total fraction [T]) and heated at 100°C for 5 min. Of the remaining portion, 800 µl was centrifuged for 20 min at 50,000 × *g* at 4°C. The lipid layer was removed, and 75 µl of the supernatant (S) was mixed with 75 µl of 2× sample buffer and heated at 100°C for 5 min. The pellet (P) was resuspended in 800 µl of lysis buffer, and 75 µl was mixed with 75 µl of 2× sample buffer and heated at 100°C for 5 min. Exocyst proteins were detected by SDS–PAGE followed by Western blotting with anti-HA mouse monoclonal antibody (Covance HA.11 clone 16B12), anti-Sec10p, or anti-Sec15p sera (Novick lab collection) at 1:1000 dilution. Control membrane protein Sso1/2p was detected with anti-Sso1/2 (1:5000) and Snc1/2p was detected with anti-Snc1/2 sera (1:1000; Novick lab collection).

Coimmunoprecipitation

One-liter cultures of yeast strains expressing flag-tagged exocyst subunits (NY3271, NY3275-3280) were grown at 25°C to OD_{600} around 1.5. For yeast strains NY3271-3274, cells were grown at 20°C and then shifted to 37°C for 2 h. Cells were then pelleted, washed once with water, and flash frozen in liquid nitrogen before storage at –80°C for future use. A mortar and pestle, prechilled with liquid nitrogen, were used to grind the cell pellet submerged in liquid nitrogen until it became a fine powder. Cells were resuspended in 5 ml of lysis buffer (20 mM PIPES [piperazine-*N*,*N*′-bis(2-ethanesulfonic acid], pH 6.8, 150 mM NaCl, 1 mM EDTA, 10% glycerol, 10 mM β-mercaptoethanol, 1 mM PMSF, 2× protease inhibitor cocktail) and then centrifuged for 2 min at 500 × *g* at 4°C. The supernatant was subjected to either ultracentrifugation or detergent solubilization followed by centrifugation. For ultracentrifugation, the lysate was transferred to tubes and subjected to 50,000 × *g* for 20 min at 4°C. The cleared cell lysate was transferred to a 15-ml Falcon tube, and NP40 was added to a 0.1% final concentration. For solubilization prior to centrifugation, NP40 was first added to the above crude cell lysate to final 0.1%, incubated at 4°C for 15 min and then subjected to 20,000 × *g* for 30 min at 4°C. Cleared cell lysates from either direct ultracentrifugation or solubilization followed by centrifugation were incubated with 80 µl 50% anti-FLAG beads slurry (Sigma) at 4°C for 2 h. Beads were washed three times with lysis buffer containing 0.5% NP40. Bound proteins were eluted by incubating with 0.5 mg/ml 3xFLAG peptide (Sigma) at 4°C for 1 h and detected by gel-code blue staining on SDS–PAGE or by Western blot with rabbit polyclonal anti-Sec3p, anti-Sec6p, anti-Sec8p, anti-Sec10p, anti-Sec15p, anti-Exo84p (Novick lab collection; 1:1000), anti-Exo70p (1:1000; provided by P. Brennwald, University of North Carolina School of Medicine, Chapel Hill, NC), anti-Adh1p (1:10,000; EMD Millipore AB1202), and mouse monoclonal anti-Flag antibody (Sigma; 1:1000).

Fluorescence microscopy

Yeast strains harboring a GFP-tag were grown at 25°C to early log phase (OD_{600} 0.4–0.6) in selective SC medium. Fluorescence imaging was performed as described previously (Liu and Novick, 2014). In brief, images were acquired with a 100× oil immersion objective lens (Plan Apochromat 100×/1.4 NA oil DIC lens; Carl Zeiss) on a spinning disk confocal microscopy system (Yokogawa Electric Corporation), which includes a microscope (Observer Z1; Carl Zeiss) equipped with an electron multiplying charge-coupled device camera (QuantEM 512SC; Photometrics). Excitation of GFP or mCherry was achieved using 488-nm argon and 568-nm argon/krypton lasers, respectively. Images were analyzed using AxioVision software 4.8 (Carl Zeiss).

Immunofluorescence

Immunofluorescence was performed as described previously with minor modifications (Pringle *et al.*, 1991). Basically, yeast strains expressing a TM-anchored exocyst subunit were grown at 25°C to early log phase (OD_{600} 0.5–0.6) in selective SC medium. Cells (about 10 ml) were harvested and then resuspended in 2 ml of phosphate-buffered formaldehyde (100 mM KPi, pH 6.5, 0.5 mM $MgCl_2$, 3.7% formaldehyde). After 2–4 h incubation at RT with gentle shaking, cells were pelleted and washed twice with 5 ml of 100 mM KPi (pH 7.5) and once with 1 ml of 100 mM KPi, pH 7.5, and 1.2 M sorbitol and resuspended in 1 ml of the above solution containing 2 µl of β–mercaptoethanol and 30 µg/ml Zymolyase 100T. Cells were incubated in a 37°C water bath for 30 min with occasional inversion. Cells were then washed three times with 100 mM KPi, pH 7.5, and 1.2 M sorbitol and finally resuspended in 1 ml of the same solution. Of the cell suspension, 10–15 µl was placed in each well of an eight-well multitest slide, which has been pretreated with polylysine. Cells were rinsed once with 1× phosphate-buffered saline (PBS) and then incubated with one drop of 1xPBS/0.5% SDS for 10 min. After five washes with PBS/bovine serum albumin, cells were blotted with anti-HA (1:1000) or anti-myc (1:1000).

Yeast vacuole staining with FM4-64

Yeast strains were grown at 25°C to early log phase (OD_{600} 0.5–0.8) in selective SC medium. Cells (about 1 ml) were harvested and then resuspended in 100 µl of YPD media with 16 µM of FM4-64. After incubation at 25°C for 1 h, cells were pelleted and washed once with 1 ml of YPD media. Cells were finally resuspended in SC medium. After ~10 min, cells were mounted and examined by fluorescence microscopy.

Invertase secretion assay

The invertase secretion assay was performed as described by Liu and Novick (2014) with minor modification. Basically, yeast cells were grown overnight at 25°C in SC medium with 5% glucose to early log phase (0.3–0.8 OD_{600}/ml). Units of cells (0.5 OD_{600}) were transferred to a 15-ml Falcon tube, pelleted, washed once with 1 ml of 10 mM NaN_3, and kept on ice. This was the 0-h sample. Another 0.5 OD_{600} units of cells were washed once with sterile water, resuspended in 1 ml of SC medium with 0.1% glucose, and incubated at 37°C with shaking for 1 h. Cells were pelleted, resuspended in 1 ml of 10 mM NaN_3, and kept on ice. This was the 1-h sample. For each 0- and 1-h sample, the external invertase was measured directly. The internal invertase was measured after cells were converted into spheroplasts, pelleted, and lysed with 0.5 ml of 0.5% Triton X-100. The fraction of invertase secreted was calculated by [Ext (1 h) – Ext (0 h)]/<[Ext (1 h) – Ext (0 h)] + [Int (1 h) – Int (0 h)]>.

Bgl2p secretion assay

The Bgl2p secretion assay was performed as described by Kozminski *et al.* (2006) with minor modification. In brief, yeast cells (30 ml) were grown at 25°C in SC medium overnight to early log phase (0.3 OD_{600}/ml). About 4.5 OD_{600} units of cells were transferred to a new flask. Two sets were prepared for each strain. One set was incubated at 25°C, and the other set was incubated at 37°C with shaking for 90 min. Cell cultures from both temperatures were

then harvested by centrifugation at 900 × *g* for 5 min. Cell pellets were resuspended in 1 ml of ice-cold 10 mM NaN_3 and 10 mM NaF, followed by a 10-min incubation on ice. The suspension was transferred to microfuge tubes, pelleted, and resuspended in 1 ml of fresh prespheroplasting buffer (100 mM Tris-HCl, pH 9.4, 50 mM β-mercaptoethanol, 10 mM NaN_3, and 10 mM NaF). After a 15-min incubation on ice, cells were pelleted and washed with 0.5 ml of spheroplast buffer (50 mM KH_2PO_4-KOH, pH 7.0, 1.4 M sorbitol, and 10 mM NaN_3). Cells were resuspended in 1 ml of spheroplast buffer containing 167 µg/ml zymolyase 100T (Nacasai Tesque Inc.). Cells were incubated in a 37°C water bath for 30 min. Spheroplasts were then pelleted at 5000 × *g* for 10 min, and 100 µl of the supernatant was transferred into a new tube and mixed with 100 µl of 2× SDS sample buffer. This was the external pool. All the remaining supernatant was removed, and the pellet (spheroplast) was rinsed once with 1 ml of spheroplast buffer and then resuspended in 200 µl of 1× SDS sample buffer. This was the internal pool. Five microliters of each intoernal pool sample (2.5% of total) and external pool sample (0.25% of total) were loaded ont a 10% SDS–PAGE gel. Bgl2p was visualized by Western blotting with anti-Bgl2p rabbit polyclonal antibody at 1:10,000 dilution (provided by R. Schekman, University of California, Berkeley, CA). The amount of Bgl2p in both internal and external pools was determined by ImageJ software. The fraction of Bgl2p accumulated was calculated by Int/(Int+Ext).

ACKNOWLEDGMENTS

We thank P. Brennwald (Department of Cell Biology and Physiology, University of North Carolina School of Medicine) for anti-Exo70p serum, R. Schekman (University of California, Berkeley) for anti-Bgl2p serum, and J. L. Brodsky (University of Pittsburgh, Pittsburgh, PA) for anti-Sec61p serum. This study was supported by grant GM35370 from the National Institutes of Health to P.N.

REFERENCES

Aalto MK, Ronne H, Keranen S (1993). Yeast syntaxins Sso1p and Sso2p belong to a family of related membrane proteins that function in vesicular transport. EMBO J 12, 4095–4104.

Abeliovich H, Grote E, Novick P, Ferro-Novick S (1998). Tlg2p, a yeast syntaxin homolog that resides on the Golgi and endocytic structures. J Biol Chem 273, 11719–11727.

Apel AR, Hoban K, Chuartzman S, Tonikian R, Sidhu S, Schuldiner M, Wendland B, Prosser D (2017). Syp1 regulates the clathrin-mediated and clathrin-independent endocytosis of multiple cargo proteins through a novel sorting motif. Mol Biol Cell 28, 2434–2448.

Bowser R, Muller H, Govindan B, Novick P (1992). Sec8p and Sec15p are components of a plasma membrane-associated 19.5S particle that may function downstream of Sec4p to control exocytosis. J Cell Biol 118, 1041–1056.

Boyd C, Hughes T, Pypaert M, Novick P (2004). Vesicles carry most exocyst subunits to exocytic sites marked by the remaining two subunits, Sec3p and Exo70p. J Cell Biol 167, 889–901.

Brennwald P, Kearns B, Champion K, Keranen S, Bankaitis V, Novick P (1994). Sec9 is a SNAP-25-like component of a yeast SNARE complex that may be the effector of Sec4 function in exocytosis. Cell 79, 245–258.

Brown FC, Pfeffer SR (2010). An update on transport vesicle tethering. Mol Membr Biol 27, 457–461.

Dong G, Hutagalung AH, Fu C, Novick P, Reinisch KM (2005). The structures of exocyst subunit Exo70p and the Exo84p C-terminal domains reveal a common motif. Nat Struct Mol Biol 12, 1094–1100.

Drees BL, Sundin B, Brazeau E, Caviston JP, Chen GC, Guo W, Kozminski KG, Lau MW, Moskow JJ, Tong A, *et al*. (2001). A protein interaction map for cell polarity development. J Cell Biol 154, 549–571.

Dubuke ML, Maniatis S, Shaffer SA, Munson M (2015). The exocyst subunit Sec6 interacts with assembled exocytic SNARE complexes. J Biol Chem 290, 28245–28256.

Finger FP, Hughes TE, Novick P (1998). Sec3p is a spatial landmark for polarized secretion in budding yeast. Cell 92, 559–571.

Finger FP, Novick P (1997). Sec3p is involved in secretion and morphogenesis in Saccharomyces cerevisiae. Mol Biol Cell 8, 647–662.

Gandhi M, Goode BL, Chan CS (2006). Four novel suppressors of gic1 gic2 and their roles in cytokinesis and polarized cell growth in Saccharomyces cerevisiae. Genetics 174, 665–678.

Guo W, Roth D, Walch-Solimena C, Novick P (1999). The exocyst is an effector for Sec4p, targeting secretory vesicles to sites of exocytosis. EMBO J 18, 1071–1080.

Guo W, Tamanoi F, Novick P (2001). Spatial regulation of the exocyst complex by Rho1 GTPase. Nat Cell Biol 3, 353–360.

Harsay E, Bretscher A (1995). Parallel secretory pathways to the cell surface in yeast. J Cell Biol 131, 297–310.

He B, Xi F, Zhang X, Zhang J, Guo W (2007). Exo70 interacts with phospholipids and mediates the targeting of the exocyst to the plasma membrane. EMBO J 26, 4053–4065.

Heider MR, Gu M, Duffy CM, Mirza AM, Marcotte LL, Walls AC, Farrall N, Hakhverdyan Z, Field MC, Rout MP, *et al*. (2016). Subunit connectivity, assembly determinants and architecture of the yeast exocyst complex. Nat Struct Mol Biol 23, 59–66.

Kozminski KG, Alfaro G, Dighe S, Beh CT (2006). Homologues of oxysterol-binding proteins affect Cdc42p- and Rho1p-mediated cell polarization in Saccharomyces cerevisiae. Traffic 7, 1224–1242.

Kushnirov VV (2000). Rapid and reliable protein extraction from yeast. Yeast 16, 857–860.

Lewis MJ, Nichols BJ, Prescianotto-Baschong C, Riezman H, Pelham HR (2000). Specific retrieval of the exocytic SNARE Snc1p from early yeast endosomes. Mol Biol Cell 11, 23–38.

Liu D, Novick P (2014). Bem1p contributes to secretory pathway polarization through a direct interaction with Exo70p. J Cell Biol 207, 59–72.

Longtine MS, McKenzie A 3rd, Demarini DJ, Shah NG, Wach A, Brachat A, Philippsen P, Pringle JR (1998). Additional modules for versatile and economical PCR-based gene deletion and modification in Saccharomyces cerevisiae. Yeast 14, 953–961.

McNew JA, Parlati F, Fukuda R, Johnston RJ, Paz K, Paumet F, Sollner TH, Rothman JE (2000). Compartmental specificity of cellular membrane fusion encoded in SNARE proteins. Nature 407, 153–159.

Morgera F, Sallah MR, Dubuke ML, Gandhi P, Brewer DN, Carr CM, Munson M (2012). Regulation of exocytosis by the exocyst subunit Sec6 and the SM protein Sec1. Mol Biol Cell 23, 337–346.

Novick P, Botstein D (1985). Phenotypic analysis of temperature-sensitive yeast actin mutants. Cell 40, 405–416.

Picco A, Irastorza-Azcarate I, Specht T, Boke D, Pazos I, Rivier-Cordey AS, Devos DP, Kaksonen M, Gallego O (2017). The in vivo architecture of the exocyst provides structural basis for exocytosis. Cell 168, 400–412e418.

Pringle JR, Adams AE, Drubin DG, Haarer BK (1991). Immunofluorescence methods for yeast. Methods Enzymol 194, 565–602.

Ren Y, Yip CK, Tripathi A, Huie D, Jeffrey PD, Walz T, Hughson FM (2009). A structure-based mechanism for vesicle capture by the multisubunit tethering complex Dsl1. Cell 139, 1119–1129.

Roumanie O, Wu H, Molk JN, Rossi G, Bloom K, Brennwald P (2005). Rho GTPase regulation of exocytosis in yeast is independent of GTP hydrolysis and polarization of the exocyst complex. J Cell Biol 170, 583–594.

Ruohola H, Ferro-Novick S (1987). Sec53, a protein required for an early step in secretory protein processing and transport in yeast, interacts with the cytoplasmic surface of the endoplasmic reticulum. Proc Natl Acad Sci USA 84, 8468–8472.

Shen D, Yuan H, Hutagalung A, Verma A, Kummel D, Wu X, Reinisch K, McNew JA, Novick P (2013). The synaptobrevin homologue Snc2p recruits the exocyst to secretory vesicles by binding to Sec6p. J Cell Biol 202, 509–526.

Stimpson HE, Toret CP, Cheng AT, Pauly BS, Drubin DG (2009). Early-arriving Syp1p and Ede1p function in endocytic site placement and formation in budding yeast. Mol Biol Cell 20, 4640–4651.

TerBush DR, Maurice T, Roth D, Novick P (1996). The Exocyst is a multiprotein complex required for exocytosis in Saccharomyces cerevisiae. EMBO J 15, 6483–6494.

TerBush DR, Novick P (1995). Sec6, Sec8, and Sec15 are components of a multisubunit complex which localizes to small bud tips in Saccharomyces cerevisiae. J Cell Biol 130, 299–312.
Tripathi A, Ren Y, Jeffrey PD, Hughson FM (2009). Structural characterization of Tip20p and Dsl1p, subunits of the Dsl1p vesicle tethering complex. Nat Struct Mol Biol 16, 114–123.
Valdez-Taubas J, Pelham HR (2003). Slow diffusion of proteins in the yeast plasma membrane allows polarity to be maintained by endocytic cycling. Curr Biol 13, 1636–1640.
Vasan N, Hutagalung A, Novick P, Reinisch KM (2010). Structure of a C-terminal fragment of its Vps53 subunit suggests similarity of Golgi-associated retrograde protein (GARP) complex to a family of tethering complexes. Proc Natl Acad Sci USA 107, 14176–14181.
Walworth NC, Novick PJ (1987). Purification and characterization of constitutive secretory vesicles from yeast. J Cell Biol 105, 163–174.
Wiederkehr A, De Craene JO, Ferro-Novick S, Novick P (2004). Functional specialization within a vesicle tethering complex: bypass of a subset of exocyst deletion mutants by Sec1p or Sec4p. J Cell Biol 167, 875–887.
Yu IM, Hughson FM (2010). Tethering factors as organizers of intracellular vesicular traffic. Annu Rev Cell Dev Biol 26, 137–156.
Yue P, Zhang Y, Mei K, Wang S, Lesigang J, Zhu Y, Dong G, Guo W (2017). Sec3 promotes the initial binary t-SNARE complex assembly and membrane fusion. Nat Commun 8, 14236.
Zhang X, Bi E, Novick P, Du L, Kozminski KG, Lipschutz JH, Guo W (2001). Cdc42 interacts with the exocyst and regulates polarized secretion. J Biol Chem 276, 46745–46750.
Zhang X, Orlando K, He B, Xi F, Zhang J, Zajac A, Guo W (2008). Membrane association and functional regulation of Sec3 by phospholipids and Cdc42. J Cell Biol 180, 145–158.